Research Square

Preprints are preliminary reports that have not undergone peer review.
They should not be considered conclusive, used to inform clinical practice,
or referenced by the media as validated information.

The interaction of a long oligocytosine mismatch in the middle of a DNA duplex with silver ions at different pH values

Andrey V. Baryshev
Saint-Petersburg State University
Nina A. Kasyanenko
Saint-Petersburg State University
Rubel A. Aleksandr
Saint-Petersburg State University
Petr A. Sokolov
p.a.sokolov@spbu.ru

Saint-Petersburg State University

Research Article

Keywords: silver, DNA, mismatch, pH, oligocytosine

Posted Date: November 23rd, 2026

DOI: https://doi.org/10.21203/rs.3.rs-11278590/v1

License: This work is licensed under a Creative Commons Attribution 4.0 International License.
Read Full License

Additional Declarations: No competing interests reported.

Abstract

DNA-based nanotechnology has immense potential and wide-ranging applications in rapidly advancing fields such as tissue engineering, drug delivery, cancer treatment, intelligent nanodevices, programmable nanomachines, biosensing, biodetection, and diagnostics. However, the thermal, chemical, and mechanical sensitivity of DNA materials limits their usability under demanding conditions. Silver-mediated base pairing is a promising solution for the specified shortcomings. In this study, we explored the incorporation of silver ions into a DNA matrix consisting of an oligocytosine interior stabilized by flanking duplexes. The effects of pH and ionic strength on silver incorporation were examined using UV and fluorescence melting, fluorescence spectroscopy, and gel electrophoresis.

1. Introduction

DNA-based nanotechnology has great potential and extensive applications in the rapidly developing fields of tissue engineering, drug delivery, cancer therapy, intelligent nanodevices, switchable nanomachines, biosensing, biodetection, and diagnostics [1]. However, the application of DNA is partly limited by the relatively weak hydrogen bonding and π-stacking interactions that maintain its structure. The resulting thermal, chemical, and mechanical fragility of DNA materials impose restrictions on the conditions under which they can be used. To overcome these limitations, new approaches to enhancing the stability of such materials are needed. One way is to exploit non-canonical metal-mediated base pairs, particularly those involving silver [2].

Silver ions are appealing because they exhibit unusually specific interactions with DNA, binding strongly to nucleobases while interacting only weakly with the negatively charged phosphate backbone [3]. This interaction is highly selective, with a 1:1 stoichiometry and a binding constant of approximately 10^6 M^{-1} [4]. Silver binding is favored at internal C/C mismatches, increases with ionic strength, and remains stable over a broad pH range (5–9), whereas higher silver concentrations (> 10 μM) can induce DNA compaction and condensation [3], [5], [6], [7]. The incorporation of C–Ag^+–C base pairs into DNA-based materials finds interesting applications in silver sensors, DNA wires, molecular switches, logic circuits, and luminescent clusters [2]. More broadly, silver-mediated base pairing provides a versatile strategy for designing robust, programmable DNA nanomaterials with enhanced stability, including under physiological conditions. From a medical perspective, silver is of great interest due to its antibacterial activity and relatively low toxicity to humans. However, soluble silver compounds are readily absorbed by the body because of their ability to bind to proteins and nucleic acids. Symptoms of chronic silver exposure include decreased blood pressure, intestinal irritation, liver and kidney damage, changes in blood cells, and the development of argyria. The growing silver-based product industry underscores the importance of understanding the cytotoxic effects of silver, including the mechanisms of silver binding to DNA.

To our knowledge, the interaction of silver ions with extended oligocytosine mismatches embedded within canonical DNA duplexes remains poorly understood. In contrast to the widely studied long

homocytosine sequences, the longest reported oligocytosine mismatches were only three [8] and six [9] consecutive C/C base pairs. The three-cytosine-long mismatch bound one to three silver ions, stabilizing the duplex, whereas excess silver led to duplex deformation. The six C–Ag^+–C base pairs were also shown to stabilize the DNA duplex, but less effectively than the imidazole–Ag^+–C analog. In the present work, we investigate the interaction of silver ions with consecutive oligocytosine mismatches 8–16 bp in length constrained by a canonical DNA duplex. We anticipate that studying such systems will advance the understanding and design of silver nanowires, silver detection devices, and switches with a wide range of response concentrations, as well as provide insight into the effects of silver on DNA in living organisms [2].

2. Methods and materials

2.1. Reagents

Milli-Q water was used to prepare all solutions except the electrophoresis buffers, which were prepared using double-distilled water. The 1×SB contained 10 mM NaOH and 40 mM boric acid (the stock solution was 25×, pH 8.5). The 1×SBAC contained 15 mM NaOH or 15 mM $NaNO_3$, 40 mM boric acid, and 10 mM sodium acetate (the stock solution was 25×, pH 8.5 when 15 mM NaOH was added or pH 5.5 when 15 mM $NaNO_3$ was added). The 1×TBTAC buffer contained 10 mM Tris, 10 mM Bis-Tris, and 10 mM sodium acetate (the stock solution was 2×; the pH was adjusted from 5.0 to 9.0 using HCl). The $AgNO_3$, $NaNO_3$ and Thiazole Orange (TO) stock solutions were 500 mM, 5 M, and 40 mM, respectively. All reagents were of analytical grade (> 99% purity) and were purchased from Dia-m (Russia).

2.2. Oligonucleotides

The oligonucleotides were purchased in lyophilized form from DNA-Synthesis (Moscow, Russia); the sequences are given in Table 1. The oligonucleotides were designed to contain consecutive C/C mismatches of different lengths in the middle and identical terminal sequences composed of adenines and thymines.

Table 1
Oligonucleotide 5'→3' sequences. Duplexes of the type x-nC-X:Y-nC-y are denoted as nCC.

x-8C-X	**AATAATAATAATTTTTCCCCCCCCTTTTTAATAATAATAA**
Y-8C-y	TTATTATTATTAAAAA**CCCCCCCC**AAAAATTATTATTATT
x-10C-X	AATAATAATAATTTTT**CCCCCCCCCC**TTTTTAATAATAATAA
Y-10C-y	TTATTATTATTAAAAA**CCCCCCCCCC**AAAAATTATTATTATT
x-12C-X	AATAATAATAATTTTT**CCCCCCCCCCCC**TTTTTAATAATAATAA
Y-12C-y	TTATTATTATTAAAAA**CCCCCCCCCCCC**AAAAATTATTATTATT
x-14C-X	AATAATAATAATTTTT**CCCCCCCCCCCCCC**TTTTTAATAATAATAA
Y-14C-y	TTATTATTATTAAAAA**CCCCCCCCCCCCCC**AAAAATTATTATTATT
x-16C-X	AATAATAATAATTTTT**CCCCCCCCCCCCCCCC**TTTTTAATAATAATAA
Y-16C-y	TTATTATTATTAAAAA**CCCCCCCCCCCCCCCC**AAAAATTATTATTATT
Y-16G-y	TTATTATTATTAAAAA**GGGGGGGGGGGGGGGG**AAAAATTATTATTATT
A20-T20	AAAAAAAAAAAAAAAAAAAATTTTTTTTTTTTTTTTTT

2.3. Sample preparation

The stock solutions of oligonucleotides were prepared by dissolving the lyophilized oligonucleotides in Milli-Q water, aliquoted into volumes required for a single measurement, and stored at − 24°C. Before measurements, the aliquots were thawed, mixed with diluted stock solutions of buffer and $AgNO_3$ and annealed by heating to 80°C, followed by slow cooling to room temperature.

2.4. Melting experiments

UV melting experiments were performed using a Specord 200 spectrophotometer equipped with a 1 cm quartz cuvette. Samples were heated at a rate of 1°C min^{-1}. Fluorescence melting experiments were performed using an AB 7500 Real-Time PCR System. Samples were heated at a rate of 0.3°C min^{-1}. The oligonucleotide concentration was 400 nM for all measurements. The buffer contribution was subtracted. The melting temperatures (T_m) were calculated as the maximum of the first derivative of the melting curve.

2.5. Electrophoresis

Samples were run in 4–5% MS-8 agarose at 1.6 V/cm for 1.5 h, followed by staining with 0.05% ethidium bromide for 30 min.

2.6. Fluorescence measurements

Thiazole Orange (TO) was used as a fluorescent probe for i-motif or duplex formation. A F-7100 spectrophotometer equipped with a 1 cm quartz cuvette was used at room temperature. The excitation wavelength was set to 488 nm. The buffer contribution was subtracted. The oligonucleotide concentration was 400 nM for all measurements.

2.7. NUPACK calculations

The T_m values of the studied oligos were evaluated using the NUPACK Python module (https://nupack.org/) [10] over a Na^+ concentration range of 50–250 mM (the lowest concentration supported by the software), using 5 mM increments. For T_m estimation at 10 mM Na^+, the dependence of T_m on sodium ion concentration was extrapolated.

3. Results and discussion

The melting temperatures of the x:y and X:Y ends of the nCC duplexes calculated using NUPACK were about 10 degrees lower than the melting temperature of the entire duplex. The consecutive oligocytosine mismatch connecting the x:y and X:Y terminal regions may either behave as an unstructured linker (modeled as a random coil in NUPACK), thereby increasing duplex stability, or adopt non-canonical conformations that either promote or hinder duplex formation. Such structures are not considered in the NUPACK model. Experimentally, at pH 8.5, we observed melting temperatures of the duplexes that were slightly lower than the corresponding NUPACK predictions, as shown in Table 2, indicating that the oligocytosine linker does not behave as a random coil and interferes with hybridization of the duplex ends. At alkaline pH, the formation of oligocytosine non-canonical structures is unlikely because the formation of i-motifs [11], C–H^+–C [12], or A–H^+–C [13] mismatch pairs requires a significant concentration of protons (i.e., conditions at pH below 7.0). In contrast, T:A:T triplexes remain stable up to pH 10.2 [14]. Sterically, the formation of triplexes by the oligonucleotide ends is possible, thereby interfering with their hybridization to yield a duplex. With that, the triplex-to-duplex transition may not manifest in UV melting curves in the absence of magnesium ions [15]. Consequently, we attribute the deviation of the calculated T_m values of nCC duplexes from the experimental values to the fact that NUPACK does not account for the formation of inter- or intramolecular triplexes. The potential formation of side structures shifts the equilibrium toward duplex dehybridization and, respectively, toward a decrease in the melting temperature.

Table 2
NUPACK-calculated (theor) and measured (exp) melting temperatures of nCC duplexes and **the** A20-T20 hairpin at pH 8.5.

Structure	**T_m, °C at 10 mM Na^+**	**T_m, °C at 100 mM Na^+**	
	theor	**theor**	**exp**
x-8C-X:Y-8C-y	27	38	31
x-10C-X:Y-10C-y	27	38	32
x-12C-X:Y-12C-y	26	37	30
x-14C-X:Y-14C-y	26	37	32
x-16C-X:Y-16C-y	26	37	36
A20-T20	50	63	62

Silver ions promote the formation of C–Ag^+–C metallo-base pairs, which may enhance the nCC duplexes stability [3]. To address whether the pre-formation of nCC duplexes is necessary for incorporation of silver ions into consecutive oligocytosine mismatches, two different synthesis protocols were applied, as shown in Fig. 1. In the first protocol, silver was added to a 1×SB (pH 8.5, 10 mM Na^+) solution containing x-nC-X:Y-nC-y oligos. In the second protocol, silver was added to a 10×SB (pH 8.5, 100 mM Na^+) solution containing x-nC-X:Y-nC-y oligos, followed by dilution to 1×SB. The first protocol did not result in the emergence of any melting transitions. This indicates that silver ions cannot trigger duplex hybridization through assembly of C–Ag^+–C pairs. It has previously been shown that oligocytosines themselves can form duplexes with each other in a parallel orientation at high ionic strength (500 mM NH_4OAc) and at high oligonucleotide concentration (5–50 μM) [16], [17], [18]. We assume that we do not observe a similar phenomenon in 1×SB (10 mM Na^+) because such a low ionic strength is insufficient to screen the DNA charge and to facilitate interaction between the oligos. Moreover, the 10–100-fold lower oligonucleotide concentration is also insufficient for the formation of intermolecular complexes. At the same time, adenines also coordinate silver, which can hinder the hybridization of the flanking ends and sequester a portion of the silver ions [18]. In contrast, samples prepared using the second protocol exhibited melting transitions, with T_m increasing as the silver-ion concentration increased. Thus, the preliminary formation of C/C mismatch matrix within the nCC duplex is a necessary step for the incorporation of silver ions into it. This is consistent with the fact that a terminal mismatch located outside the DNA B-duplex region cannot bind a silver ion [5]. Alternatively, one might hypothesize that the tenfold increase in oligonucleotide concentration in the second protocol before dilution could lead to the formation of parallel sequential C–Ag^+–C metal-mediated base pairs. This is unlikely, however, as it would require either duplex dehybridization and strand flipping or formation of a complex between several duplexes, neither of which we observed in other experiments.

We compared the influence of silver ions on the completely complementary duplex x-16C-X:Y-16G-y (16GC) and the duplex containing a consecutive oligocytosine mismatch, 14CC, using electrophoresis.

The results are presented in Fig. 2. It was suggested that long G/C [18], [19] or A/T [18], [20] runs can form regions with Ag^+-mediated metallo-pairs. In our case, this is unlikely, since silver ions had no significant effect on the mobility of the complementary duplex, which contains both G:C and A:T base pairs. In contrast, a change in the electrophoretic mobility of the 14CC duplex indicates the interaction of silver ions with its oligocytosine mismatch. The decrease in band intensity with increasing silver concentration may be attributed to impaired staining of metalated DNA with ethidium bromide. Taking into account the results of the melting experiments shown in Fig. 1B, it can be assumed that interstrand C–Ag^+–C metallated pairs are formed. It should also be noted that no additional bands appear when silver is added. We can therefore conclude that neither denaturation of the duplex into individual strands nor the formation of higher-order structures takes place. It is important to note that DNA–silver complexes exhibit considerable polymorphism. For instance, silver can form intrastrand C–Ag^+–C pairs rather than interstrand ones. In that case, no difference would be expected in the data shown in Fig. 1. However, the coexistence of the intrastrand and interstrand C–Ag^+–C variants at comparable concentrations is possible.

We systematically investigated the effect of silver ions on the thermodynamics of duplexes differing only in the length of the oligocytosine mismatch (nCC duplexes) at alkaline pH. All considered duplexes showed similar changes in their melting profiles upon addition of silver nitrate. We did not observe a smooth change in the duplex T_m, as previously reported for C/C or CCC/CCC mismatches [3], [8]. Instead, as the amount of silver increased, the low melting temperature (T_{low}) near 32°C gradually vanished, while a higher melting temperature (T_{high}) near 47°C emerged, as shown in Fig. 3A. Using the 10CC duplex as an example, we demonstrated that above a ratio of 1 Ag^+ ion per 1 C/C mismatch, significant changes ceased and saturation was observed, taking into account that excess silver interacts with adenines at the flanking ends. This indicates silver binding specifically to the oligocytosine regions, accompanied by the formation of C–Ag^+–C metal-mediated base pairs (**Figure S1**). To quantitatively describe these changes, we calculated the areas under the peaks of the first derivatives corresponding to the vanishing (S_{low}) and emerging (S_{high}) melting transitions, as shown in Fig. 3A **(inset)**. The derivatives of each melting curve were fitted with two Gaussians, and the areas and positions of the maxima were taken as S_{low} or S_{high} and T_{low} or T_{high}, respectively. At silver concentrations below 0.5 Ag^+ per 1 C/C mismatch, only a subtle inflection in the melting curve was observed in the 47°C region. Given the correspondingly small S_{high} area under the derivative curve, we attribute this feature to an artifact of curve processing. For all duplexes, the S_{low} area decreased and the S_{high} area increased upon addition of silver, as shown in Fig. 3B. We assume that the incorporation of silver ions into the duplex induces an internal rearrangement of its structure. This rearrangement leads to the destabilization of the x:y and X:Y ends, manifested as an increase in the optical density at low temperatures. At the same time, silver-mediated cytosine pairs are formed, manifested by the emergence of a higher melting transition, as shown in Fig. 3C. The formation of Ag-mediated non-Watson-Crick A-Ag^+-T base pairs is unlikely. Silver exhibits high specificity for unpaired cytosines, and there is no excess silver available to form complexes with A/T pairs at the concentrations used. The melting data indicate the cooperative binding of silver and

the existence of two fractions of duplexes, with and without incorporated silver ions. Previously, the cooperative silver binding to natural DNA was reported only at silver concentrations greater than 10 μM [7], [21] or for modified base pairs [22]. In our experiments, the concentration was lower, and the electrophoresis data do not show two distinct bands corresponding to these fractions of duplexes (with and without incorporated silver ions). Further clarification is therefore required.

We employed the Thiazole Orange (TO) dye, which binds both duplexes and i-motifs [23], [24] and carries a positive charge [25], to investigate DNA conformations at different pH values. At pH 8.5, a transition near 32°C was observed, as shown in Fig. 4A, in good agreement with the UV melting profile of the duplex without silver addition. As shown in Fig. 4B, at a corresponding ratio of 0.5 TO per A/T base pair in 100 mM Na^+ the fluorescence of the 16CC duplex is comparable to that of the A20-T20 hairpin and significantly greater than the signal for the duplex in 10 mM Na^+ (where stable duplexes are not formed, as shown in Fig. 1A). It can therefore be concluded that the primary fluorescence enhancement results from dye intercalation into A/T base pairs rather than from binding to the oligocytosine region or non-hybridized flanking ends. At high TO concentrations in 100 mM Na^+, the fluorescence of the duplex becomes significantly lower than that of the hairpin. This may be due to binding of the dye without fluorescence enhancement to the oligocytosine region. At the same time, the shape of the TO spectrum changes for the 16CC duplex and tends toward the corresponding spectrum of single-strand-bound TO at low ionic strength, as shown in Fig. 4C. Previously, this spectral alteration was correlated with dimerization [26] or aggregation [27] of TO. We suppose that single-stranded regions can promote such aggregation under the conditions used.

At pH 5.5, a new structure with a melting transition at approximately 50°C was observed at fluorescence melting curves; this transition was not observed for individual strands or under low-salt conditions (**Figure S2**). We associate this phenomenon with the duplex-assisted formation of an interstrand i-motif or C–H^+–C base pairs [28], [29] within the oligocytosine mismatch. Moreover, the stability of such structures is comparable to that manifested in UV melting at pH 8.5 with silver, which may indicate a similar mechanism of interior mismatch stabilization by protons and Ag^+ ions. Agreeably, the TO fluorescence increased markedly with decreasing pH in 10 mM Na^+ as shown in **Figure S3** and Fig. 4B. It can be concluded that single-stranded oligocytosine regions can also form inter- or intramolecular i-motif structures under acidic conditions, which is in good agreement with previously reported data [11]. Under low-salt conditions, the signal decreased with increasing dye concentration. This decay can be attributed to the predominance of non-fluorescent dye-binding modes, the destabilization of the i-motif, or dye aggregation at high concentrations. For the A20-T20 hairpin in 100 mM Na^+, the fluorescence intensity decreased on average relative to that at high pH, which can be explained by the protonation and destabilization of A/T base pairs. Because the dye and protons are similarly charged, the protonation may reduce the affinity of TO for DNA. For the duplex, on the contrary, the fluorescence increased slightly, which may be associated with the formation of additional binding sites on the i-motif. There was no signal decay upon increasing TO concentration under high-salt conditions. It can therefore be concluded that dehybridization of A/T base pairs followed by the formation of single-stranded conformations does not occur. At pH 5.5, the shape of the spectrum for the A20-T20 hairpin changes similarly to that

observed at high pH. For the duplex, the change in spectral shape at low pH relative to high pH is consistent with the appearance of new binding sites on the inter- or intramolecular i-motifs at 100 mM or 10 mM Na^+, respectively.

Next, we considered the competition between silver ions and protons for binding to cytosines engaged in i-motif constitution at low pH. Consistent with the fluorescence melting data, the UV melting curves exhibit a single transition around 50°C, as shown in Fig. 5A. In terms of shape and position, this transition closely matches the one observed at pH 8.5 upon addition of 1 Ag^+ ion per 1 C/C mismatch. Meanwhile, as shown in Fig. 5B, at low pH and in the absence of silver, the position of the maximum and the absorbance at 305 nm undergo a hypsochromic shift and a decrease in intensity, respectively, as the temperature rises—changes characteristic of i-motifs [30], [31]. Upon addition of 1 Ag^+ ion per 1 C/C mismatch, the melting temperature decreases slightly, the transition at 305 nm disappears, and the maximum undergoes a bathochromic shift. We attribute this to disruption of the intermolecular i-motif within the duplex and formation of C–Ag^+–C base pairs, similar to the behavior observed at high pH. Doubling the silver concentration, as at high pH (Figure S1), does not lead to any further significant changes. This supports the conclusion that the i-motif is generally incompatible with formation of C–Ag^+–C base pairs [32].

4. Conclusions

In this paper, we demonstrate that pre-formation of the DNA matrix consisting of an oligocytosine interior stabilized by flanking duplexes is a necessary condition for binding of silver ions and assembly of consecutive C–Ag^+–C mismatch base pairs. We examined interiors formed by two oligocytosine sequences, each 8–16 nucleotides long, with unmodified flanking duplexes consisting of 16 A/T base pairs. Incorporation of silver ions did not result in dehybridization of the duplexes, regardless of the length of the oligocytosine segments; instead, C–Ag^+–C mismatch base pairs were formed. The melting data indicate cooperative binding of silver ions. However, given the possible polymorphism of DNA–silver complexes, this conclusion requires further verification by independent methods.

This work also provides new insights into the assembly of i-motifs under the constraints imposed by flanking duplexes. Our fluorescence studies suggest that intermolecular i-motif formation within the duplex interior occurs at high ionic strength upon decreasing pH. In contrast, when the flanking duplexes are unstable, intramolecular i-motif formation becomes possible. We assume that silver ions successfully compete with protons for binding within the oligocytosine interior at low pH. Therefore, we speculate that formation of long C–Ag^+–C mismatch base pairs at acidic pH is generally possible when stable flanking duplexes provide structural constraints.

We anticipate that studying the interaction between long oligocytosine mismatches located within DNA duplexes and silver ions across different pH values may support the rational design and optimization of various DNA-based nanostructures, ranging from molecular switches to metallized DNA-based systems.

Our findings may also contribute to the development of pH sensors and drug-delivery strategies targeting cancerous tissues, where local acidification frequently occurs.

Declarations

Funding

The authors acknowledge Saint-Petersburg State University for a research project 161726507.

Authors' contribution

S.P.A.: conception and design of the work; acquisition, interpretation, and analysis of data; critical revision for important intellectual content; drafted the manuscript;

B.A.V.: acquisition and analysis of data; interpretation and analysis of data; drafted the manuscript;

R.*A*.A.: interpretation of data;

K.N.A.: interpretation of data; critical revision of the manuscript for important intellectual content.

Acknowledgements

We acknowledge Maria A. Popova for essential details that facilitated the experimental conditions search. The authors thank the SPbU Laboratory of Amyloid Biology for providing the apparatus to conduct fluorescence melting experiments.

References

1. W. Ma, Y. Zhan, Y. Zhang, C. Mao, X. Xie, and Y. Lin, "The biological applications of DNA nanomaterials: current challenges and future directions," *Sig Transduct Target Ther*, vol. 6, no. 1, p. 351, Oct. 2021, doi: 10.1038/s41392-021-00727-9.
2. Q. Sun, X. Xie, Y. Song, and L. Sun, "A review on silver-mediated DNA base pairs: methodology and application," *Biomater Res*, vol. 26, no. 1, p. 9, Sep. 2022, doi: 10.1186/s40824-022-00254-w.
3. A. Ono *et al.*, "Specific interactions between silver(i) ions and cytosine–cytosine pairs in DNA duplexes," *Chem. Commun.*, no. 39, p. 4825, 2008, doi: 10.1039/b808686a.
4. H. Torigoe, I. Okamoto, T. Dairaku, Y. Tanaka, A. Ono, and T. Kozasa, "Thermodynamic and structural properties of the specific binding between Ag+ ion and C:C mismatched base pair in duplex DNA to form C–Ag–C metal-mediated base pair," *Biochimie*, vol. 94, no. 11, pp. 2431–2440, Nov. 2012, doi: 10.1016/j.biochi.2012.06.024.
5. H. Torigoe and H. Kida, "Specific binding of Ag+ to central C C mismatched base pair but not terminal C C pair in duplex DNA," *Thermochimica Acta*, vol. 738, p. 179770, Aug. 2024, doi: 10.1016/j.tca.2024.179770.

6. Y. Wang, B. Ritzo, and L.-Q. Gu, “Silver(i) ions modulate the stability of DNA duplexes containing cytosine, methylcytosine and hydroxymethylcytosine at different salt concentrations,” *RSC Adv.*, vol. 5, no. 4, pp. 2655–2658, 2015, doi: 10.1039/C4RA14490B.
7. W.-Y. Jiang and S.-Y. Ran, “Two-stage DNA compaction induced by silver ions suggests a cooperative binding mechanism,” *The Journal of Chemical Physics*, vol. 148, no. 20, p. 205102, May 2018, doi: 10.1063/1.5025348.
8. M. N. Hossain, S. Ahmad, and H. Kraatz, “Consecutive Silver(I) Ion Incorporation into Oligonucleotides containing Cytosine-Cytosine Mispairs,” *ChemPlusChem*, vol. 86, no. 2, pp. 224–231, Feb. 2021, doi: 10.1002/cplu.202000607.
9. J. C. Léon, D. González-Abradelo, C. A. Strassert, and J. Müller, “Fluorescent DNA-Templated Silver Nanoclusters from Silver(I)-Mediated Base Pairs,” *Chemistry A European J*, vol. 24, no. 33, pp. 8320–8324, Jun. 2018, doi: 10.1002/chem.201801858.
10. M. E. Fornace, N. J. Porubsky, and N. A. Pierce, “A Unified Dynamic Programming Framework for the Analysis of Interacting Nucleic Acid Strands: Enhanced Models, Scalability, and Speed,” *ACS Synth. Biol.*, vol. 9, no. 10, pp. 2665–2678, Oct. 2020, doi: 10.1021/acssynbio.9b00523.
11. S. Benabou, A. Aviñó, R. Eritja, C. González, and R. Gargallo, “Fundamental aspects of the nucleic acid i-motif structures,” *RSC Adv.*, vol. 4, no. 51, pp. 26956–26980, 2014, doi: 10.1039/C4RA02129K.
12. J. SantaLucia and R. Kierzek, “Stabilities of Consecutive A C , C C , GoG, UC,and UmU Mismatches in RNA Internal Loops: Evidence for Stable Hydrogen-Bonded U4J and C C + Pairsf”.
13. J. D. Puglisi, J. R. Wyatt, and I. Tinoco, “Solution conformation of an RNA hairpin loop,” *Biochemistry*, vol. 29, no. 17, pp. 4215–4226, May 1990, doi: 10.1021/bi00469a026.
14. A. Idili, A. Vallée-Bélisle, and F. Ricci, “Programmable pH-Triggered DNA Nanoswitches,” *J. Am. Chem. Soc.*, vol. 136, no. 16, pp. 5836–5839, Apr. 2014, doi: 10.1021/ja500619w.
15. C. Gondeau, “Circular dichroism and UV melting studies on formation of an intramolecular triplex containing parallel T*A:T and G*G:C triplets: netropsin complexation with the triplex,” *Nucleic Acids Research*, vol. 26, no. 21, pp. 4996–5003, Nov. 1998, doi: 10.1093/nar/26.21.4996.
16. S. M. Swasey, F. Rosu, S. M. Copp, V. Gabelica, and E. G. Gwinn, “Parallel Guanine Duplex and Cytosine Duplex DNA with Uninterrupted Spines of Ag^{I} -Mediated Base Pairs,” *J. Phys. Chem. Lett.*, vol. 9, no. 22, pp. 6605–6610, Nov. 2018, doi: 10.1021/acs.jpclett.8b02851.
17. S. M. Swasey and E. G. Gwinn, “Silver-mediated base pairings: towards dynamic DNA nanostructures with enhanced chemical and thermal stability,” *New J. Phys.*, vol. 18, no. 4, p. 045008, Apr. 2016, doi: 10.1088/1367-2630/18/4/045008.
18. S. M. Swasey, L. E. Leal, O. Lopez-Acevedo, J. Pavlovich, and E. G. Gwinn, “Silver (I) as DNA glue: Ag+-mediated guanine pairing revealed by removing Watson-Crick constraints,” *Sci Rep*, vol. 5, no. 1, p. 10163, May 2015, doi: 10.1038/srep10163.
19. T. Lenz, U. Javornik, M. Hebenbrock, J. Plavec, and J. Müller, “Determination of silver(I)-binding sites in canonical B-DNA by NMR spectroscopy,” *J Biol Inorg Chem*, vol. 30, no. 4, pp. 381–395, Aug. 2025, doi: 10.1007/s00775-025-02115-y.

20. E. Bethur, Z. Zhao, R. Guha, H. Zeng, and S. M. Copp, “Assembly and solution phase properties of Ag^+-mediated adenine–thymine DNA duplexes,” *Inorg. Chem. Front.*, p. 10.1039.D5QI01833A, 2026, doi: 10.1039/D5QI01833A.
21. J. Hao, D. Cao, Q. Zhao, D. Zhang, and H. Wang, “Intramolecular Folding of PolyT Oligonucleotides Induced by Cooperative Binding of Silver(I) Ions,” *Molecules*, vol. 27, no. 22, p. 7842, Jan. 2022, doi: 10.3390/molecules27227842.
22. K. Petrovec, B. J. Ravoo, and J. Müller, “Cooperative formation of silver(i)-mediated base pairs,” *Chem. Commun.*, vol. 48, no. 97, p. 11844, 2012, doi: 10.1039/c2cc36169h.
23. B. H. Kang, Z. F. Gao, N. Li, Y. Shi, N. B. Li, and H. Q. Luo, “Thiazole orange as a fluorescent probe: Label-free and selective detection of silver ions based on the structural change of i-motif DNA at neutral pH,” *Talanta*, vol. 156–157, pp. 141–146, Aug. 2016, doi: 10.1016/j.talanta.2016.05.006.
24. O. Suss, L. Motiei, and D. Margulies, “Broad Applications of Thiazole Orange in Fluorescent Sensing of Biomolecules and Ions,” *Molecules*, vol. 26, no. 9, p. 2828, May 2021, doi: 10.3390/molecules26092828.
25. S. Ikeda and A. Okamoto, “pH-dependent fluorescence of uncharged benzothiazole-based dyes binding to DNA”.
26. J. Nygren, N. Svanvik, and M. Kubista, “The interactions between the fluorescent dye thiazole orange and DNA,” *Biopolymers*, vol. 46, no. 1, pp. 39–51, Jul. 1998, doi: 10.1002/(SICI)1097-0282(199807)46:1<39::AID-BIP4>3.0.CO;2-Z.
27. S. Dutta Choudhury, A. C. Bhasikuttan, H. Pal, and J. Mohanty, “Surfactant-Induced Aggregation Patterns of Thiazole Orange: A Photophysical Study,” *Langmuir*, vol. 27, no. 20, pp. 12312–12321, Oct. 2011, doi: 10.1021/la202414h.
28. D. M. Gray, T. Cui, and R. L. Ratliff, “Circular dichroism measurements show that C.C+ base pairs can coexist with A.T base pairs between antiparallel strands of an oligodeoxynucleotide double-helix.,” *Nucleic Acids Res*, vol. 12, no. 19, pp. 7565–7580, Oct. 1984, doi: 10.1093/nar/12.19.7565.
29. T. Brown, G. A. Leonard, E. D. Booth, and G. Kneale, “Influence of pH on the conformation and stability of mismatch base-pairs in DNA,” *Journal of Molecular Biology*, vol. 212, no. 3, pp. 437–440, Apr. 1990, doi: 10.1016/0022-2836(90)90320-L.
30. J.-L. Mergny, L. Lacroix, X. Han, J.-L. Leroy, and C. Helene, “Intramolecular Folding of Pyrimidine Oligodeoxynucleotides into an i-DNA Motif,” *J. Am. Chem. Soc.*, vol. 117, no. 35, pp. 8887–8898, Sep. 1995, doi: 10.1021/ja00140a001.
31. E. P. Wright, J. L. Huppert, and Z. A. E. Waller, “Identification of multiple genomic DNA sequences which form i-motif structures at neutral pH,” *Nucleic Acids Res*, vol. 45, no. 6, pp. 2951–2959, Apr. 2017, doi: 10.1093/nar/gkx090.
32. V. Seiffert *et al.*, “Are i-Motif Structures in DNA Compatible with Cytosine–Ag(I)–Cytosine Base Pairs?,” *Angewandte Chemie International Edition*, vol. n/a, no. n/a, p. e19809, doi: 10.1002/anie.202519809.

Figures

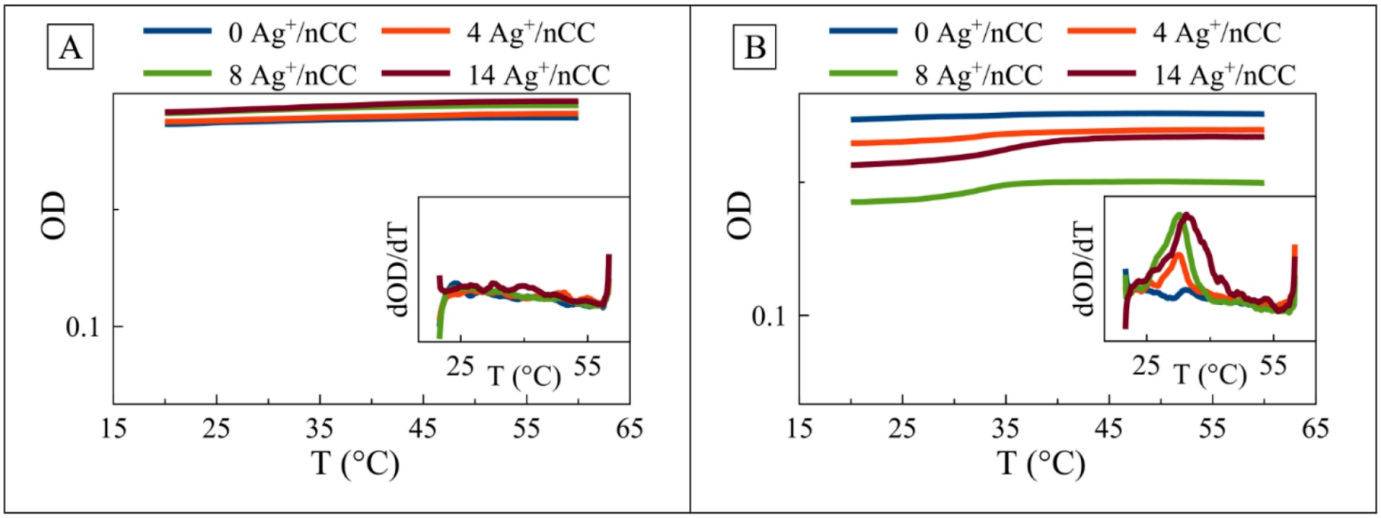


Figure 1

Dependence of OD on temperature (melting curves) and the corresponding first derivatives for a 1×SB (pH 8.5, 10 mM Na^+) solution containing x-14C-X and y-14C-Y oligos at a 1:1 ratio, prepared under different conditions: silver ions were added in 1×SB (A) or in 10×SB (pH 8.5, 100 mM Na^+), followed by dilution to 1×SB (B).

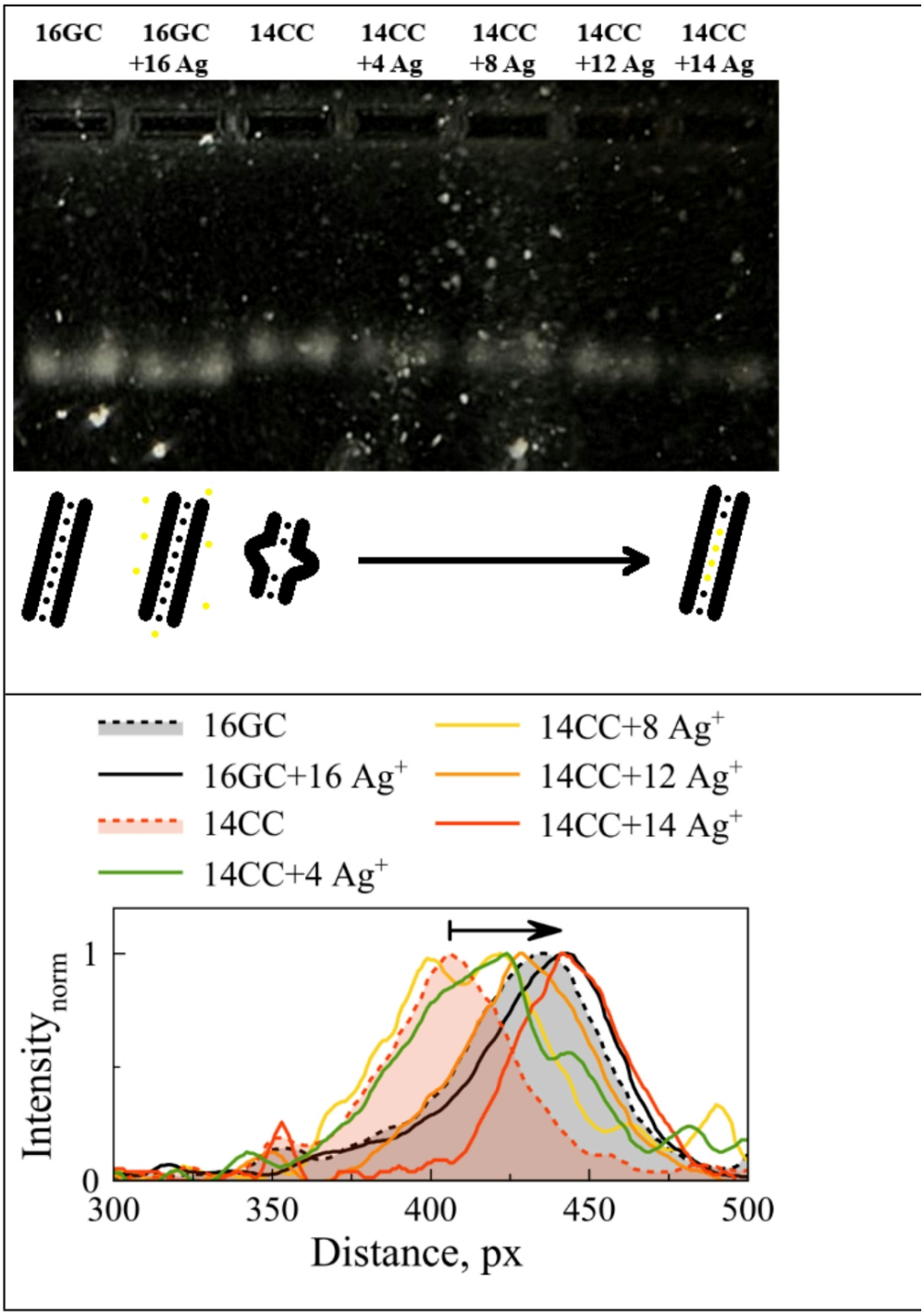


Figure 2

Electropherogram of the x-16C-X:Y-16G-y (16GC) and x-14C-X:Y-14C-y (14CC) duplexes in 10×SB (pH 8.5, 100 mM Na^+), with and without silver ions, and the corresponding electrophoretic mobility.

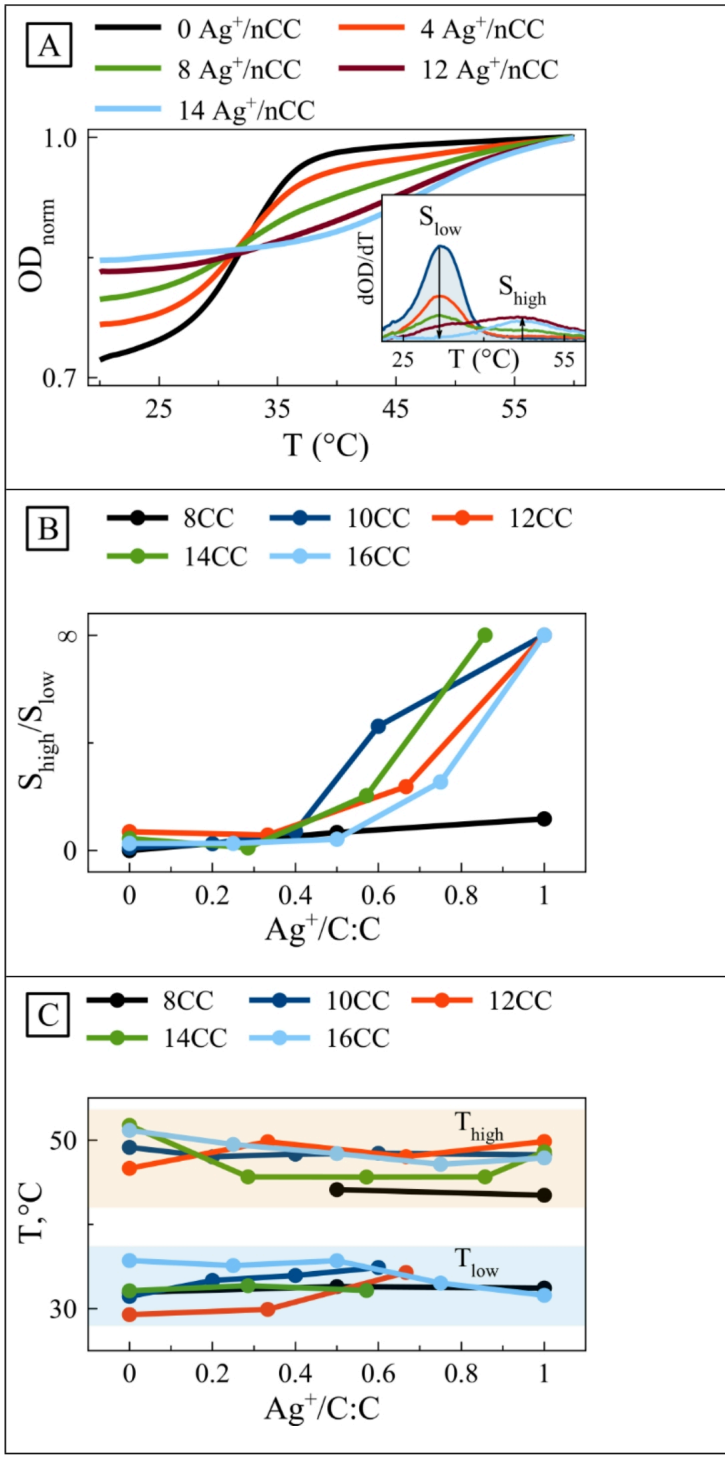


Figure 3

UV melting curves of **the 14CC** duplex with different amounts of silver ions in **10×SB (pH** 8.5, 100 mM Na^+) and **the** corresponding first derivative (A). **Dependence** of S_{low}/S_{high} (B) and T_{low}, T_{high} (C) on **the Ag^+-per-**C/C mismatch ratio.

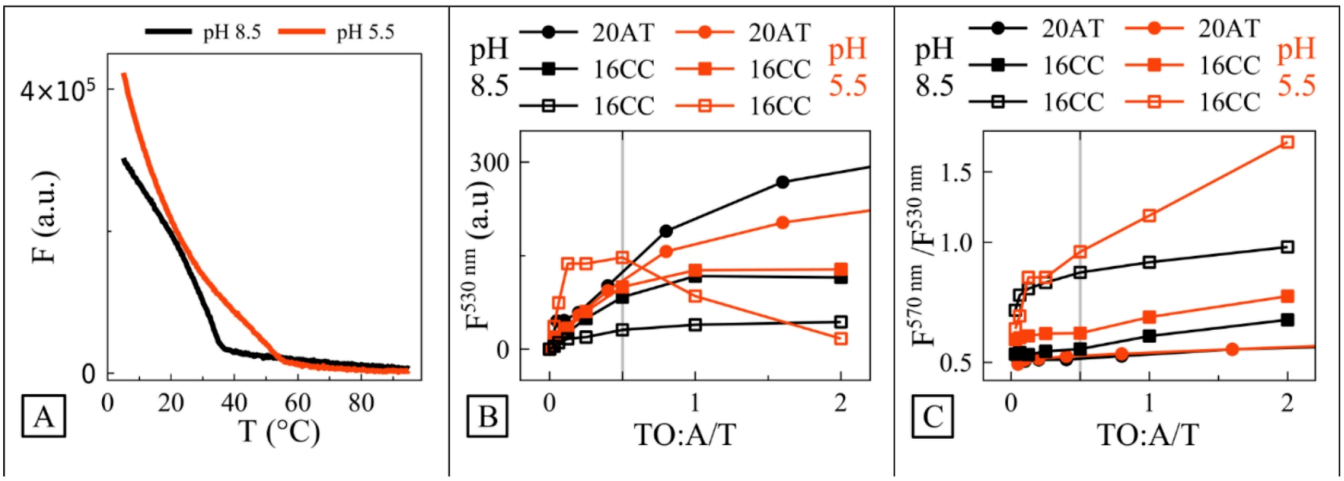


Figure 4

TO (0.5 molecules per A/T base pair) fluorescence melting curves of the 12CC duplex in 100 mM Na^+ at pH 8.5 and 5.5 (A). Dependence of TO fluorescence intensity per A/T base pair at 530 nm on its concentration for the A20-T20 hairpin and 16CC duplex at pH 8.5 and pH 5.5 in 100 mM (black and red) or 10 mM Na^+ (green) (B). Corresponding ratio of fluorescence intensity at 530 nm to fluorescence intensity at 570 nm (C). 1×SBAC and 0.4×SBAC buffer concentrations were employed to prepare 100 mM and 10 mM Na^+ solutions. The spectrum of the dye without DNA was subtracted.

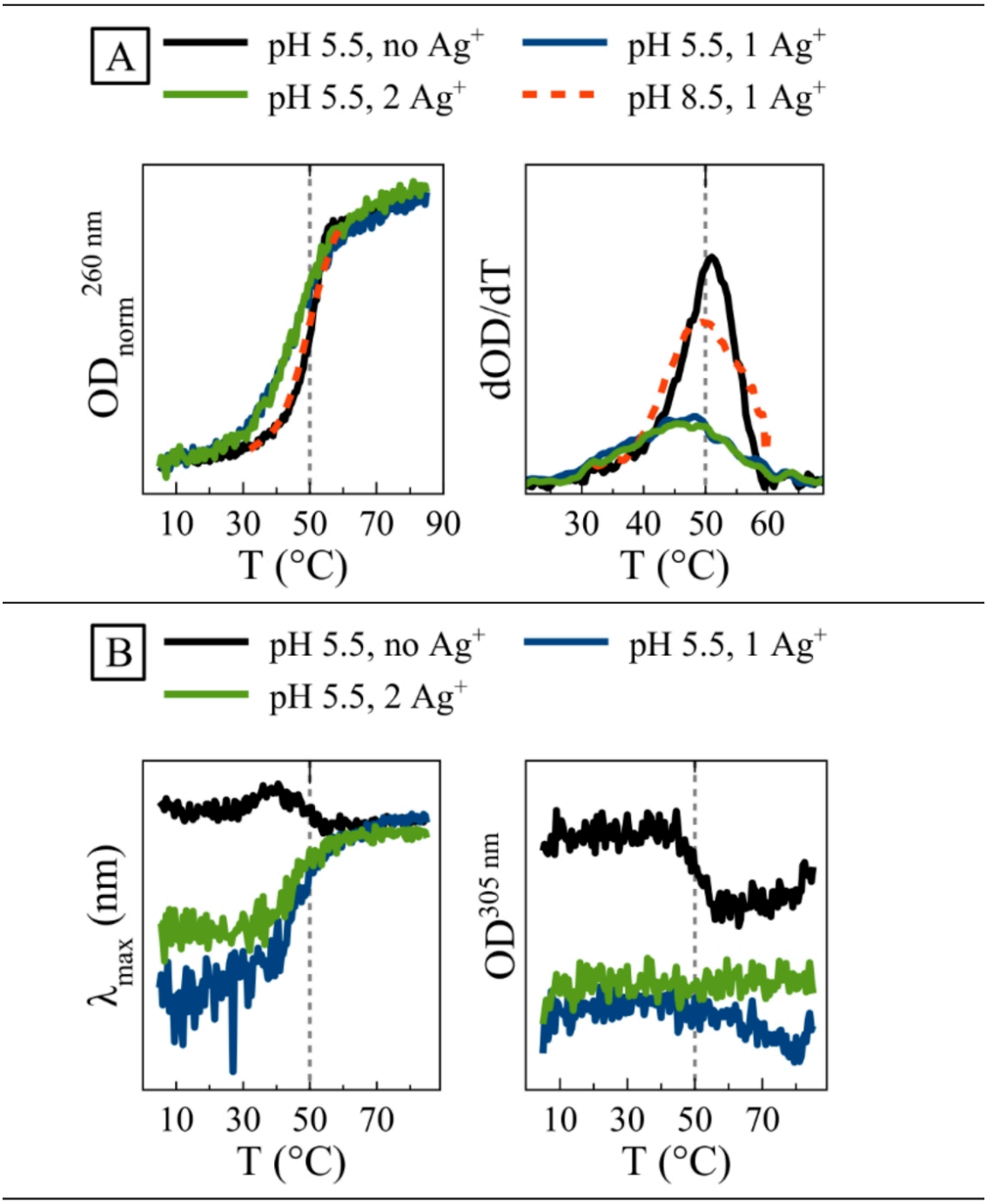


Figure 5

UV melting curves of the 12CC duplex with different silver-ion-to-C/C-base-pair ratios in 1×SBAC (pH 5.5, 100 mM Na^+) or 10×SB (pH 8.5, 100 mM Na^+) at 260 nm or 305 nm and the corresponding first derivative and maximum absorbance position.

Supplementary Files

This is a list of supplementary files associated with this preprint. Click to download.

- SI.docx